Institut de Physique
Université de Neuchâtel

Dynamique de phase près du seuil de percolation de réseaux supraconducteurs désordonnés

Forme réduite de la thèse

présentée à la Faculté des Sciences
de l'Université de Neuchâtel
pour l'obtention du grade de docteur ès sciences

par
Ali-Laurent Eichenberger
physicien diplômé
de l'Université de Neuchâtel

Neuchâtel, octobre 1997.

IMPRIMATUR POUR LA THÈSE

Dynamique de phase près du seuil de percolation de réseaux supraconducteurs désordonnés

de M. Ali-Laurent Eichenberger

UNIVERSITÉ DE NEUCHÂTEL

FACULTÉ DES SCIENCES

La Faculté des sciences de l'Université de Neuchâtel sur le rapport des membres du jury,

Mme A.-C. Mota (ETH Zürich),
MM. P. Martinoli (directeur de thèse), H. Beck,
et B. Pannetier (CNRS, Grenoble)

autorise l'impression de la présente thèse.

Neuchâtel, le 5 novembre 1997

Le doyen:

F. Stoeckli

Liste des publications

- A.-L. Eichenberger, J. Affolter, M. Willemin, M. Mombelli, H. Beck, P. Martinoli and S.E. Korshunov, Phys. Rev. Lett. **77**, 3903 (1996).

- A.-L. Eichenberger, J. Affolter, M. Willemin, Ch. Leemann and P. Martinoli, Czechoslovak Journal of Physics (Proceedings of the LT21 Conference) **46 suppl. S2**, 697 (1996).

- B. Pannetier, A. Bezryadin and A.-L. Eichenberger, Physica **B 222**, 253 (1996).

- B. Pannetier, A. Eichenberger, Lebanese Scientific Research Reports **1**, 28 (1996).

Le texte complet de la thèse est déposé dans le bureau du professeur Piero Martinoli à l'Institut de Physique de l'Université de Neuchâtel.

Dynamic Measurement of Percolative Critical Exponents in Disordered Josephson Junction Arrays

A.-L. Eichenberger, J. Affolter, M. Willemin, M. Mombelli, H. Beck, and P. Martinoli
Institut de Physique, Université de Neuchâtel, Ch-2000 Neuchâtel, Switzerland

S. E. Korshunov
L. D. Landau Institute for Theoretical Physics, Kosygina 2, 117940 Moscow, Russia
(Received 25 June 1996)

The complex conductance $G(\omega)$ of site-diluted Josephson junction arrays close to the percolation threshold was measured over a wide range of frequencies ω. Well below T_c both the superfluid [$\omega \mathrm{Im}G$] and dissipative [$\mathrm{Re}G$] components are independent of ω below a critical frequency ω_c, whereas $G(\omega) \propto \omega^{-u}$ with $u \approx \frac{1}{2}$ for $\omega > \omega_c$. This is shown to reflect the crossover from a Euclidean regime ($\omega < \omega_c$) dominated by phononlike modes of the phase system to a fractal regime ($\omega > \omega_c$), where the relevant excitations are localized fractons. Percolative critical exponents extracted from the data are consistent with theoretical predictions. [S0031-9007(96)01507-4]

PACS numbers: 74.50.+r, 63.50.+x, 64.60.Ak, 74.80.–g

Percolation is the simplest idea to understand a disordered system. Near the percolation threshold, percolating systems exhibit a natural self-similar structure with geometrical inhomogeneities occurring over a broad range of length scales and are therefore conveniently described in terms of fractal geometry [1]. With regard to superconductivity, fractal and percolation concepts have proven very useful in acquiring insight into the physics of granular superconductors [2–8]. Although a number of investigations have been performed on disordered granular materials, in most cases the structural aspects of their randomness are so poorly known that a detailed comparison with theoretical predictions is almost impossible. With the advent of modern microfabrication techniques, however, it has become possible to investigate model systems, such as Josephson junction arrays and superconducting wire networks, where both the nature and the amount of disorder can be accurately controlled. Early work has focused on the superconducting-to-normal phase boundary of percolating wire networks exposed to a magnetic field [9,10]. More recently, a Berezinskii-Kosterlitz-Thouless (BKT) transition has been shown to persist in randomly diluted Josephson junction arrays in zero field [11], whereas the unusual scaling properties of vortices as well as the effect of field-induced frustration on superconducting phase coherence have been investigated in a deterministic fractal lattice (the Sierpinski gasket) sharing essential geometrical elements with a truly percolating system near threshold [12,13].

Almost no attention has been paid so far to the *dynamics* of the phase degrees of freedom associated with the randomly distributed superconducting islands in a disordered array. In this Letter we report a study, covering five decades in driving angular frequency ω, of the linear complex ac sheet conductance $G(\omega, p, T)$ of site-diluted triangular arrays of proximity-effect coupled Josephson junctions with site occupation probabilities p very close to the percolation threshold p_c. By exploring the response as a function of ω in zero magnetic field (i.e., at zero frustration) and at temperatures where thermally created vortices are irrelevant, we observe, at a critical value ω_c, a remarkable crossover from a low-frequency ($\omega < \omega_c$) regime, where both $\omega \mathrm{Im}G(\omega)$ (the inverse sheet kinetic inductance measuring superconducting phase coherence in the system) and $\mathrm{Re}G(\omega)$ (the component measuring dissipation) are independent of ω, to a high-frequency ($\omega > \omega_c$) behavior, where $G(\omega) \propto \omega^{-u}$ with $u \approx \frac{1}{2}$. Our theoretical interpretation strongly supports the idea that the crossover in response, observed at $\omega = \omega_c$, reflects the profound change in phase dynamics occurring when $l(\omega)$, the frequency-dependent length scale at which we are probing the system in the conductance measurements, becomes of the order of the percolation correlation length ξ_p [1]. For $l(\omega) > \xi_p$ (i.e., for $\omega < \omega_c$) the array is in the two-dimensional (2D) Euclidean (or homogeneous) regime, where the response is dominated by extended "phononlike" modes of the phase system similar to those occurring in an ordered 2D lattice. In contrast, for $l(\omega) < \xi_p$ (i.e., for $\omega > \omega_c$) the array is in the fractal regime, where localized "fractonlike" phase excitations lead to anomalous dynamics [1,14]. A further unusual feature emerging from our experiments is that the (expected) depression of $\omega \mathrm{Im}G(\omega, p, T)$ caused by percolative disorder is accompanied by additional dissipation, as demonstrated by the discovery of a contribution to $\mathrm{Re}G(\omega, p, T)$ which grows stronger and stronger as $p \rightarrow p_c$.

Quite generally, in the classical overdamped limit of interest in this study the sheet conductance of a Josephson junction array follows from a two-fluid description of the system in which the superfluid and the normal fluid are associated, respectively, with the sheet kinetic inductance

0031-9007/96/77(18)/3905(4)$10.00

L and the sheet resistance R of the array:

$$G = (i\omega L)^{-1} + R^{-1}. \quad (1)$$

Let us first consider an unfrustrated regular ($p = 1$) triangular array driven by a small ac current at temperatures well below the BKT transition temperature T_c. Using a resistively shunted junction model, it is straightforward to show that for $T \ll T_c$, i.e., at temperatures where the phase differences $\{\phi_{jk}(t)\}$ across the junctions are small and, consequently, only plane "phase waves" (the "spin waves" of the classical XY model isomorphic to the array) are the relevant excitations of the system, the array is equivalent to a lattice whose bonds consist of the junction inductance $L_J(T) = (\hbar/2e)^2 J^{-1}(T)$, where $J(T)$ is the temperature-dependent Josephson coupling energy, connected in parallel to the junction resistance $R_J(T)$. Then, it is readily shown that $L = L_J/\sqrt{3}$ and $R = R_J/\sqrt{3}$ for a regular triangular array.

The essential features of the dynamic response of arrays with *percolative disorder* are most easily understood in terms of bond percolation. According to the "universality hypothesis," the main conclusions drawn from this description should also be valid for site percolation (the type of disorder actually present in our samples) on *any* 2D lattice. If one assumes that Josephson couplings $\{J_{jk}\}$ only involve nearest-neighbor pairs $\langle jk \rangle$ of superconducting islands, then bond disorder amounts to set $J_{jk} = J$ on a fraction p of the bonds and $J_{jk} = 0$ on the remaining portion $(1 - p)$. The suppression of a bond $\langle jk \rangle$ also affects the corresponding resistance R_{jk}. However, randomness in the $\{R_{jk}\}$ can hardly be expected to be of any relevance in arrays of proximity-effect coupled junctions, the shunting resistance of the junctions being always finite because of the underlying normal-conducting substrate. Thus, at low enough temperatures (where vortex excitations can be ignored), an array of proximity-effect coupled junctions with bond disorder can be modeled by a two-component random network with elements having conductances $G_1 = (1/i\omega L_J) + (1/R_J)$ and $G_2 = 1/R_J$ with, respectively, probabilities p and $(1 - p)$.

To calculate the sheet conductance $G(\omega, p)$ of the system, we focus on the critical region near p_c relevant to our experiments and consider first of all the case $p = p_c$. Since ξ_p diverges at the percolation threshold, the array is in the fractal regime at all frequencies for $p = p_c$ and, consequently, $G(\omega)$ is expected to obey a power law, $G(\omega) \propto \omega^{-u}$, reflecting the dynamic scaling resulting from the self-similar structure of the system. The dynamical critical exponent u follows by noticing that, because of the self-duality of the problem, the conductance can be calculated exactly [15,16] for bond percolation on a square 2D lattice: $G = (G_1 G_2)^{1/2}$. Substituting the expressions for G_1 and G_2, we then obtain in the limit $\omega\tau_J \ll 1$ of interest ($\tau_J = L_J/R_J$ is the phase relaxation time)

$$L^{-1} = c_L L_J^{-1} (\omega\tau_J)^{1-u}, \qquad R = c_R R_J (\omega\tau_J)^u, \quad u = 1/2, \quad (2)$$

where c_L and c_R are numerical coefficients of order unity depending on the structural details of the lattice.

Above p_c, ξ_p is finite and Eq. (2) is no longer valid at all frequencies. Below some crossover frequency ω_c, we must recover the 2D homogeneous regime where both L^{-1} and R are expected to be length scale independent, i.e., independent of ω. Using general scaling arguments [1,17], near p_c the conductance can be written as $G = (G_1 G_2)^{1/2} S(z)$, where $S(z)$ is a complex scaling function and z a scaling variable proportional to $(p - p_c)(G_1/G_2)^{1/2t}$ with t the conductivity exponent [1]. At low frequencies, in the 2D Euclidean regime corresponding to $|z| \gg 1$ or, equivalently, to $\omega\tau_J \ll (p - p_c)^{2t}$, $S(z) \propto z^t(1 + \text{const} \times z^{-2t})$ [17]. Then, denoting by $L_0(p)$ and $R_0(p)$ the sheet kinetic inductance and the sheet resistance in the limit $\omega \to 0$, we find

$$L_0^{-1}(p) = c_L' L_J^{-1} (p - p_c)^t, \qquad R_0(p) = c_R' R_J (p - p_c)^t, \quad (3)$$

where c_L' and c_R' are again numerical factors of order unity depending on the lattice structure. Notice that this result is consistent with the loss of superconducting phase coherence ($L_0^{-1} = 0$) and the formation of the infinite superconducting cluster ($R_0 = 0$) at p_c.

Since the 2D-fractal dynamic crossover is expected to occur for $|z| \sim 1$, using Eq. (3) we obtain the following estimate of ω_c:

$$\omega_c \sim (p - p_c)^{2t}/\tau_J \sim R_0(p)/L_0(p). \quad (4)$$

The crossover at ω_c reflects the drastic change in phase dynamics at the transition from the low-frequency ($\omega < \omega_c$) 2D Euclidean regime, characterized by extended phononlike modes of the phase degrees of freedom, to the high-frequency ($\omega > \omega_c$) fractal regime where localized fractonlike modes are the dominant phase excitations. Calculations [18] based on a self-consistent effective medium approximation [19] reproduce, quite remarkably, the correct value of u and lead to a dynamic behavior similar to that described by Eqs. (2)–(4), however, with $t = 1$.

To test these predictions, we have measured, using a sensitive SQUID-operated two-coil mutual inductance technique [13,20] covering a wide range of driving frequencies (0.1 Hz–20 kHz), the sheet conductance of two site-diluted triangular arrays of proximity-effect coupled Pb/Cu/Pb junctions with percolation fractions $p = 0.55$ and $p = 0.51$ close to the threshold $p_c = 0.50$ [1] and normal-state junction resistances $R_N \approx 7m\Omega$ ($p = 0.55$) and $R_N \approx 3m\Omega$ ($p = 0.51$). Their inverse sheet kinetic inductances at 0.5 Hz, a frequency well below ω_c, are shown in Fig. 1(a) as a function of temperature. Because of their 2D nature at 0.5 Hz, both arrays exhibit, as demonstrated by superfluid drops consistent with the 2D universal prediction [11], a BKT transition at a temperature $T_c(p)$ whose features will be discussed in detail elsewhere. To analyze the superfluid depression caused

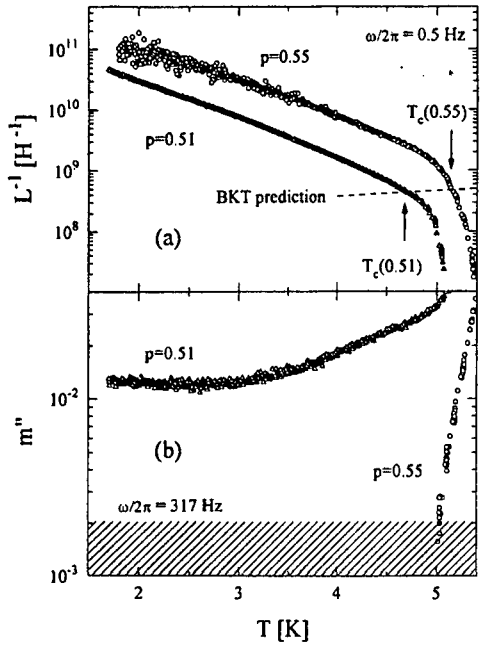

FIG. 1. Temperature dependence of (a) the inverse sheet kinetic inductance at 0.5 Hz and (b) the normalized dissipative component of the mutual inductance change at 317 Hz for two disordered arrays with different percolation fractions on a semilog plot. In (a), the dashed line is the universal prediction for the Berezinskii-Kosterlitz-Thouless transition. In (b), the shaded area is below the sensitivity threshold of the mutual inductance measurements.

by disorder below the critical region, we notice that, below $T_c(p)$, the $L^{-1}(T,p)$ curves manifestly display the same temperature dependence, thereby showing [see Eq. (3)] that the junction inductances $L_J(T) \equiv L_J(0)f(T)$ in both samples differ only in their values $L_J(0)$ at $T = 0$. Then, recalling that $L_J(0) \propto R_N$ [21], the superfluid ratio $L^{-1}(T,0.55)/L^{-1}(T,0.51) \approx 4.1$ extracted from Fig. 1(a) can be matched to that given by Eq. (3) by choosing $t \approx 1.4$, in good agreement with the prediction $t \approx 1.3$ for percolation in two dimensions [1].

To illustrate the importance of disorder with regard to dissipation, in Fig. 1(b) we show the temperature dependence of the dissipative component m'' of the mutual inductance change at 317 Hz (still below ω_c) directly detected by the SQUID and caused by the screening currents flowing in the arrays below $T_c(p)$ (m'' is normalized to the purely inductive mutual inductance change at the transition of a perfectly diamagnetic sample). Using a simplified analytical treatment of our measuring technique [20], it can be shown that, well below $T_c(p)$, $m'' \approx CL_J(T)(\omega\tau_J)(R_J/R)^3$ where C is a calibration constant of the order of 10^9 H^{-1}. Since $L_J \approx 0.1$–1 pH and $\tau_J \approx 10^{-7}$–10^{-8} s in the temperature range of interest, at 317 Hz m'' turns out to be ~5 orders of magnitude below our sensitivity threshold ($m'' \approx 0.2\%$, corresponding to an inductance sensitivity of ~1 pH) for a regular array ($R_J/R \approx 1$), whereas for our disordered samples near p_c [$R_J/R_0 \propto (p - p_c)^{-t}$ for $\omega < \omega_c$, see Eq. (3)] m'' should still be below threshold for $p = 0.55$, but well above it (about an order of magnitude) for $p = 0.51$. These predictions are consistent with the low-temperature results shown in Fig. 1(b) which demonstrate the dramatic growth [$\propto(p - p_c)^{-3t}$] of m'' in percolative arrays as $p \to p_c$. We attribute this effect to the scattering of phase (or "spin") waves in a medium whose periodicity is broken by disorder.

The central results of this paper, shown in Figs. 2 and 3, relate to the frequency dependence of G at temperatures well below $T_c(p)$, where our discussion in terms of random networks applies. In Fig. 2 we show, on a log-log plot and at three different temperatures, both $L^{-1}(\omega)$ and $R(\omega)$ over the whole frequency range accessible to our experiments for the array closer to the percolation threshold ($p = 0.51$). The $L^{-1}(\omega)$ data exhibit, at ~1 kHz, a marked crossover from a frequency-independent regime below 1 kHz to a power-law behavior $L^{-1}(\omega) \propto \omega^{(1-u)}$ with $u \approx 0.5$ above 1 kHz. This observation is clearly consistent with the behavior predicted by Eqs. (2) and (3). Although taken, in part, at the limit of our sensitivity and thus lacking the degree of precision achieved in the measurements of the superfluid component, the resistive data $R(\omega)$ also show, at about the same frequency, a crossover consistent with the model predictions, however, with a somewhat larger exponent ($u \approx 0.7$) in the fractal regime. Notice that $R(\omega)$ is strongly temperature dependent, thereby reflecting the reduction of $R_J(T)$ with decreasing temperature caused by the expanding

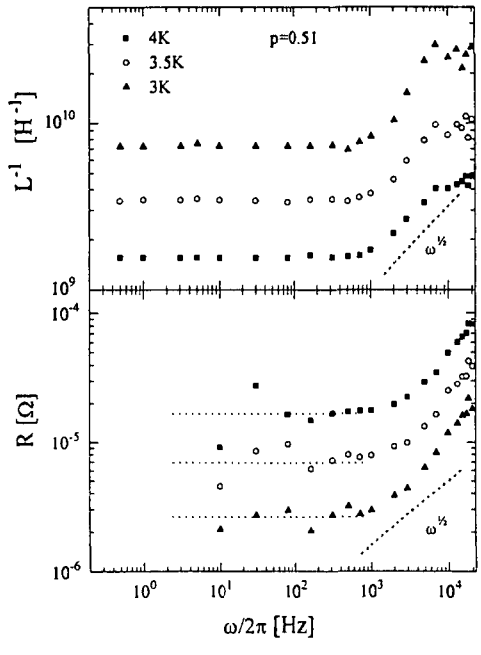

FIG. 2. Frequency dependence of the inverse sheet kinetic inductance L^{-1} and of the sheet resistance R at three different temperatures well below the critical region for the disordered array with $p = 0.51$ on a log-log plot. The dashed lines are $\sqrt{\omega}$ power laws. The dotted lines are guides to the eye to identify the low-frequency plateaus of $R(\omega)$.

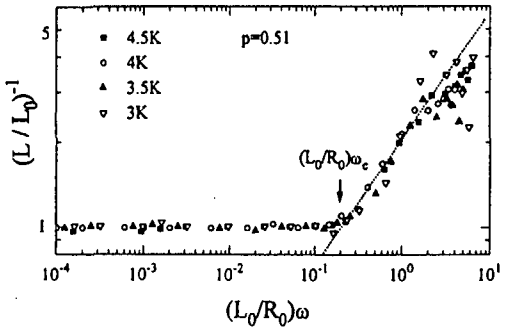

FIG. 3. Normalized inverse sheet kinetic inductance vs normalized angular frequency on a log-log plot showing the universal nature of the phonon-fracton dynamic crossover at $(L_0/R_0)\omega_c$ for the disordered array with $p = 0.51$. The dotted line is a power law with an exponent $1 - u = 0.45$ [Eq. (2)].

superconductivity in the normal Cu link of the Pb/Cu/Pb junctions. Remarkably, the temperature dependence of $R_J(T)$ turns out to be very similar to that of $L_J(T)$, thereby making $\tau_J(T)$ only weakly temperature dependent.

To stress the universal character of the "phonon-fracton" crossover, in the log-log plot of Fig. 3 we show, as a function of the scaling variable $(L_0/R_0)\omega \sim \omega/\omega_c \sim |z|^{-1}$, the normalized inverse sheet kinetic inductance $(L/L_0)^{-1}$ calculated from a collection of data taken at four different temperatures on the sample with $p = 0.51$. $L_0(T)$ and $R_0(T)$ were extracted from the low-frequency plateaus of $L^{-1}(\omega)$ and $R(\omega)$ (see Fig. 2). Within experimental accuracy, all the data collapse on a single curve, thereby demonstrating the scaling of $(L/L_0)^{-1}$ with ω/ω_c predicted by the model [Eqs. (2)–(4)]. From the power-law behavior in the high-frequency fractal regime we deduce $u = 0.55 \pm 0.07$, a value consistent with the theoretical prediction. Moreover, the crossover occurs at $(L_0/R_0)\omega_c \approx 0.2$, a value compatible with the estimate $[(L_0/R_0)\omega_c \approx 1]$ provided by Eq. (4), which entirely neglects numerical factors.

In conclusion, a study of the complex sheet conductance of site-diluted Josephson junction arrays near the percolation threshold has provided novel insight into phase dynamics and dissipative processes in disordered superconductors. In particular, by probing the arrays over a wide range of length scales, we have found strong evidence for a crossover from a low-frequency two-dimensional Euclidean regime, where the response is dominated by extended phononlike modes of the superconducting phase, to a high-frequency fractal regime, where the relevant phase excitations are localized fracton modes. Percolative critical exponents inferred from the analysis of the data are found to be consistent with theoretical predictions.

We thank Ch. Leemann for clarifying discussions and critical comments. This work was supported by the Swiss National Science Foundation.

[1] For a general review, see, *Fractal and Disordered Systems*, edited by A. Bunde and S. Havlin (Springer-Verlag, Berlin, 1991).
[2] P. G. de Gennes, C. R. Acad. Sci. Paris **292**, II-9 (1981).
[3] M. J. Stephen, Phys. Lett. **87A**, 67 (1981).
[4] S. Alexander and E. Halevi, J. Phys. (Paris) **44**, 53 (1983).
[5] C. Ebner and D. Stroud, Phys. Rev. B **28**, 5053 (1983).
[6] S. John and T. C. Lubensky, Phys. Rev. B **34**, 4815 (1986).
[7] J. Simonin and A. Lopez, Phys. Rev. Lett. **56**, 2649 (1986).
[8] S. Roux and A. Hansen, Europhys. Lett. **5**, 473 (1988).
[9] J. M. Gordon *et al.*, Phys. Rev. Lett. **59**, 2311 (1987).
[10] R. G. Steinmann and B. Pannetier, Europhys. Lett. **5**, 559 (1988).
[11] D. C. Harris *et al.*, Phys. Rev. Lett. **67**, 3606 (1991).
[12] R. Meyer *et al.*, Phys. Rev. Lett. **67**, 3022 (1991).
[13] S. E. Korshunov *et al.*, Phys. Rev. B **51**, 5914 (1995).
[14] S. Alexander and R. Orbach, J. Phys. Lett. **43**, L625 (1982).
[15] A. M. Dykhne, Zh. Eksp. Teor. Fiz. **59**, 110 (1970) [Sov. Phys. JETP **32**, 63 (1971)].
[16] J. P. Straley, Phys. Rev. B **15**, 5733 (1977).
[17] A. L. Efros and B. I. Shklovskii, Phys. Status Solidi B **76**, 475 (1976).
[18] M. Mombelli, H. Beck, and S. E. Korshunov (unpublished).
[19] B. Derrida *et al.*, Phys. Rev. B **29**, 6645 (1984).
[20] B. Jeanneret *et al.*, Appl. Phys. Lett. **55**, 2336 (1989).
[21] K. K. Likharev, Rev. Mod. Phys. **51**, 101 (1979).

LT 21

Proceedings of the 21st International Conference on Low Temperature Physics
Prague, August 8-14, 1996
Part S2 - Superconductivity 1: LTS - Tunnelling phenomena, etc.

Phase dynamics in percolating Josephson junction arrays

A. Eichenberger, J. Affolter, M. Willemin, Ch. Leemann and P. Martinoli

Institut de Physique, Université de Neuchâtel, CH-2000 Neuchâtel, Switzerland

The temperature-dependent helicity modulus $\Gamma(T)$ of site-diluted triangular arrays of proximity-effect coupled Pb/Cu/Pb Josephson junctions has been extracted from measurements of the complex ac sheet conductance performed in the frequency range 0.1 Hz to 20 kHz in zero magnetic field. At low frequencies $\Gamma(T)$ exhibits the characteristic superfluid drop predicted by the Kosterlitz-Thouless theory, demonstrating that a disordered array behaves like a homogeneous two-dimensional system at length scales larger than the percolation correlation length.

There is a fairly detailed understanding, in terms of the vortex unbinding idea put forward by the Kosterlitz-Thouless (KT) theory [1], of the critical behavior of regular unfrustrated two-dimensional (2D) Josephson junction arrays. The question of whether a KT transition still exists in arrays with strong percolative disorder is more delicate and has been addressed only in a limited number of papers [2-4]. Relying on a sensitive mutual inductance technique [5], in this letter we report a study of superconducting phase coherence in site-diluted triangular arrays of proximity-effect coupled Pb/Cu/Pb junctions with percolation fractions p very close to the percolation threshold p_c=0.50. We find that percolative disorder reduces both the strength $\Gamma(p)$ and the onset temperature $T_c(p)$ of global superconducting phase coherence in the system. Moreover, under certain conditions, the transition at $T_c(p)$ is found to be consistent with the universal scaling prediction of the KT theory.

Two length scales appear to be relevant for vortex dynamics in a disorderd system [6]: the percolation correlation length $\xi_p \propto (p-p_c)^{-\nu}$ and the frequency-dependent vortex diffusion length $r_D(\omega)$. At high angular frequencies ω, such that $r_D<\xi_p$, the array is in a fractal regime where vortices exhibit unusual scaling properties [7]. In contrast, for $r_D>\xi_p$ vortex excitations move essentially in a uniform (or euclidian) 2D system where their energy depends logarithmically on the sample size. The effective Josephson coupling energy J_R of the system, however, is renormalized by disorder. A simple analogy with a periodic triangular lattice of Sierpinski gaskets, where the gasket side is identified with ξ_p, shows [7, 8] that J_R is related to the temperature-dependent coupling energy of an individual junction J(T) by $J_R=(a/\xi_p)^{\zeta}J \propto J(p-p_c)^t$, where t is the conductivity exponent for percolation in two dimensions, a the lattice constant and $\zeta=t/\nu$. Thus, in the 2D regime in which we are primarily interested here, an array with percolative disorder is expected to exhibit a KT transition at a reduced temperature $\tau_c(p)\equiv k_BT_c(p)/J[T_c(p)]$ given by:

$$\tau_c(p)=\tau_c(1)[(p-p_c)/(1-p_c)]^t \qquad (1)$$

where $\tau_c(1)\approx 1.5$ is the reduced critical temperature of a regular (p=1) triangular array [9].

In order to test these conjectures, we have measured the inverse sheet kinetic inductance $L^{-1}(T)$ of two arrays with p=0.55 and p=0.51 over a wide range of driving frequencies (0.1 Hz-20 kHz) using a SQUID-operated two-coil technique [5]. Although $L^{-1}(T)$ provides a direct probe of the areal superfluid density and, therefore, of the degree of phase coherence in the system, for the sake of comparison, the data were analyzed in terms of a normalized quantity: the "dynamical" helicity modulus defined by $\Gamma(\tau, p, \omega)=(\sqrt{3}/2)L^{-1}(\tau, p, \omega)/L_J^{-1}(\tau)$. The single-junction inductance $L_J(\tau)=(\phi_o/2\pi)^2/J(\tau)$ (ϕ_o is the flux quantum) was inferred from measurements of the array's low-frequency response at temperatures well below T_c where $L^{-1}(\tau, p, \omega)=\sqrt{3}[(p-p_c)/(1-p_c)]^tL_J^{-1}(\tau)$. Taking the numerical prediction $t\approx 1.3$ [6], the result of the analysis performed on both samples is shown in Fig. 1 where Γ is plotted as a function of the reduced temperature τ in the low-frequency 2D regime ($r_D>\xi_p$) and in the high-frequency ($r_D<\xi_p$) fractal limit. The vortex diffusion length was estimated by observing that in euclidian systems $r_D(\omega)$ obeys the law of classical diffusion and can therefore be written as $r_D(\omega)=(\mu k_BT/\omega)^{1/2}$ where the 2D vortex mobility μ can be expressed in terms of the normal-state sheet resistance R_n and of ξ_p

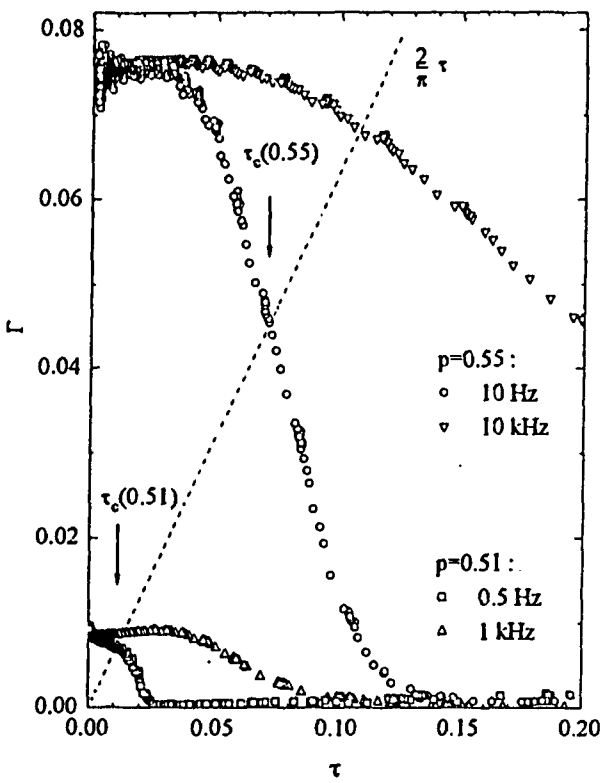

Fig. 1: Helicity modulus vs reduced temperature for two arrays with different percolation fractions. Two-dimensional critical behavior consistent with the KT scaling prediction is observed at 0.5 Hz and 10 Hz.

as $\mu=R_n\xi_p^2/\phi_o^2$. Notice that, since ξ_p is the shortest length scale consistent with 2D behavior, it is ξ_p [and not a as in the ordered case (p=1)], which enters the expression of μ. Since R_n is essentially the sheet resistance (a few mΩ) of the Cu layer providing the coupling between the Pb islands, the frequency (defined by the condition $r_D(\omega)\approx\xi_p$) at which the crossover from the homogeneous 2D behavior to the fractal regime is expected to occur is of the order of ~1 kHz near T_c.

We first notice that, over the whole frequency range covered by our experiments, growing percolative disorder, as measured by decreasing values of $(p-p_c)$, not only increasingly depresses Γ (this feature is intrinsic to our analysis, see the discussion above), but also the transition temperature which is well below that [$\tau_c(1)\approx1.5$] of the regular (p=1) array in the static thermodynamic limit (ω=0) [9].

We next focus on the critical region of the low-frequency superfluid response. According to the universal scaling prediction of the KT theory, for an infinite sample the static (ω=0) helicity modulus is expected to jump discontinously from $\Gamma(\tau_c, p)=(2/\pi)\tau_c(p)$ to zero at $\tau_c(p)$. At the finite length scales probed in our experiments, a superfluid jump no longer occurs and the transition broadens. At the lowest frequencies, however, the universal KT prediction, as shown in Fig. 1, can nevertheless be used to approximately locate $\tau_c(p)$ in the 2D regime. We find $\tau_c(0.55)\approx0.072$ and $\tau_c(0.51)\approx0.011$. Both values are consistent with Eq. (1) if one takes $t=1.32$ and $t=1.26$ respectively, in good agreement with the critical exponent ($t\approx1.3$) predicted for the conductivity percolation problem in two dimensions [6]. This observation provides convincing evidence for the KT interpretation of the transition of disordered arrays in the 2D regime.

In the fractal regime at high frequencies, the transitions become very broad and shift to higher temperatures reflecting the "hardening" of J_R at length scales shorter than ξ_p [7]. Detailed investigations of the frequency dependence of Γ in this interesting regime are in progress.

We would like thank H. Beck, S.E. Korshunov and M. Mombelli for stimulating discussions. This work was supported by the Swiss National Science Foundation.

References

[1] J.M. Kosterlitz and D.J. Thouless, J. Phys. C 6 (1973) 1181.
[2] D.C. Harris, S.T. Herbert, D. Stroud, and J.C. Garland, Phys. Rev. Lett. 67 (1991) 3606.
[3] X.C. Zeng, D. Stroud, and J.S. Chung, Phys. Rev. B 43 (1991) 3042.
[4] Ya. M. Blanter, Yu. E. Lozovik, and A. Yu. Morozov, Physica Scripta 52 (1995) 237.
[5] B. Jeanneret, J.L. Gavilano, G.A. Racine, Ch. Leemann, and P. Martinoli, Appl. Phys. Lett. 55 (1989) 2336.
[6] For a general review, see, *Fractal and Disorderd Systems*, edited by A. Bunde and S. Havlin (Springer-Verlag, Berlin, 1991).
[7] R. Meyer, J.L. Gavilano, B. Jeanneret, R. Théron, Ch. Leemann, H. Beck, and P. Martinoli, Phys. Rev. Lett. 67 (1991) 3022.
[8] S.E. Korshunov, R. Meyer, and P. Martinoli, Phys. Rev. B 51 (1995) 5914.
[9] W.Y. Shih and D. Stroud, Phys. Rev. B 32 (1985) 158.

Reprinted from

PHYSICA B
CONDENSED MATTER

Physica B 222 (1996) 253–259

Imaging of vortices in 2D superconducting arrays: Magnetic decoration and other methods

B. Pannetier[a,*], A. Bezryadin[a], A. Eichenberger[b]

[a]*Centre de Recherches sur les Très Basses Températures, associé à l'UJF, CNRS, BP 166, 38042 Grenoble-Cédex 9, France*
[b]*Institut de Physique, Rue Bréguet, CH-2000 Neüchatel, Switzerland*

ELSEVIER

ELSEVIER

Physica B 222 (1996) 253–259

PHYSICA B

Imaging of vortices in 2D superconducting arrays: Magnetic decoration and other methods

B. Pannetier[a,*], A. Bezryadin[a], A. Eichenberger[b]

[a]*Centre de Recherches sur les Très Basses Températures, associé à l'UJF, CNRS, BP 166, 38042 Grenoble-Cédex 9, France*
[b]*Institut de Physique, Rue Bréguet, CH-2000 Neûchatel, Switzerland*

Abstract

Direct observation of vortex configurations has been in the last years an interesting challenge to understanding frustration, coherence and interaction effects in superconducting arrays. Recently, magnetic decoration technique has been used to image vortices in wire arrays. The vortex configuration was found to depend strongly on the frustration. Large domains of commensurate states were observed near low rational frustration. We discuss the observed patterns in terms of the models of ground state vortex configurations in classical arrays. With increasing the width of the wires the frustration effect disappears. We present new results on multiquanta vortices in an array of microholes and an extension of this method to various superconducting arrays. A brief review is given on the recent developments on vortex imaging by other direct methods, mostly scanning probes microscopy, which gives access to dynamical properties of vortices.

1. Introduction

Vortices and charges are the elementary excitations in superconducting arrays. Most of fundamental properties of these systems are related to the ground state and dynamical states of elementary excitations. Considerable progresses have been made in the description and understanding of Josephson arrays as model systems and recent advances in fabrication and refined instrumentation open the route to new kind of microscopic observations such as vortex imaging in artificial arrays. We present here recent observations of the vortex ground state in superconducting arrays and we illustrate this review with new results on vortex decoration in various superconducting networks.

* Corresponding author.

2. Vortex imaging in superconducting arrays

Superconducting arrays are particular examples of type II superconductors with controllable parameters. A large variety of imaging methods have been developed recently for high T_c materials. With the exception of scanning tunnel microscope [1, 2] which probes the local electronic density of states. most methods rely on the observation of quantized flux lines. The magnetic decoration was the first method of imaging vortices [3] and has proved to be very powerful despite obvious limitation due to its simplicity. As a single shot experiment it is not expected to provide information on dynamics. This method has been widely used in the early days of high T_c studies (see for example Gammel et al. [4], review by Bishop et al. [5]). An elegant application was the recent experiment showing vortex

0921-4526/96/$15.00
PII S0921-4526(96)00202-5

correlations in a bulk superconductor by simultaneous observation of the decoration patterns on the two faces of the same crystal [6]. Impressive progress has been made very recently on the scanning SQUID microscopy [7]. Magnetic force microscopy is now able to image vortices in high T_c [8]. Electron holography and Lorentz microscopy were successful both in high T_C and low T_C materials [9].

The array geometry imposes specific requirements. One is due to the patterned structure which makes difficult contact scanning tunnel measurement such as scanning tunnel microscopy. In addition, tunnelling experiments are not expected to probe vortex location in arrays since the energy gap is uniform in the array. Only phase is changed in the vicinity of a vortex site. Another serious difficulty comes from the nature of vortices in arrays [10]. Because of the absence of core, the field contrast is very weak. The cell size is large, typically 1–20 μm. The magnetic field ϕ_0/A^2 is then orders of magnitude smaller than that inside the core of a type II vortex ϕ_0/λ^2 ($\lambda \approx 0.1$ μm). Also superconducting arrays are in the weak coupling regime, i.e. the effective penetration depth $\lambda_{\text{eff}} \approx \phi_0/I_C$, (Josephson junctions where I_C is the critical current) or $\lambda^2 s/a$ (wire networks: here s is the cross-section area and a the lattice spacing) is usually much larger than the unit cell a. As a consequence the flux quantum of an isolated vortex is spread over many cells. While the point-like location of the vortex is well defined [11] as the barycenter of the superconducting phase, the magnetic field profile is smooth and does not represent faithfully the vortex pattern in particular when the vortex density is large.

In contrast to the Josephson junction arrays, the strongly coupled wire network leads to a favorable situation: at low temperatures, λ becomes smaller than the width of the superconducting strands and the magnetic screening can take place at the scale of the individual cell. Magnetic field contrast, defined as the relative variation of magnetic field in cells with and without a vortex, larger than 60% has indeed been realized [12]. If shielding is large then it is convenient to describe the vortex in terms of a superconducting loop current.

3. Illustration of the decoration method

We present here some new illustrations of the decoration method in various kind of arrays. In our previous experiments the effort was made to maximize the magnetic field contrast near the superconducting network. High-quality epitaxial niobium film grown on sapphire substrates were patterned by e-beam lithography and reactive ion etching in order to reach magnetic contrast of order of a mT. Also a planarization layer was used to intercept the magnetic particles at about 0.2 μm above the plane of the network. Excellent pictures were obtained this way [12] but unfortunately the technical parameters (temperature, pressure, working distances, etc.) were so sharp that method turned out to be inappropriate for systematic observations. More recently we have developed a new approach based on a flux compression method [13]. In this method an additional superconducting layer placed underneath the array turns the coreless vortices formed in the array into Abrikosov vortices much easier to decorate with magnetic particles. Practically the preparation technique consists in interrupting the ion etching before completion in order to keep a residual niobium layer of finite thickness – about 60 nm – in the bottom of the cells. Specific requirements are needed in order to control the nucleation process. Ideally the bottom layer must have a critical temperature smaller than the critical temperature of the array. Nucleation of superconductivity in "blind hole" networks has been studied both experimentally and theoretically in Ref. [13]. Preferential nucleation of surface superconductivity at the edge of the holes at nonzero magnetic field ensures that localized quantized currents appear prior to the bulk transition temperature in field cooling experiments. The situation is similar for wire arrays although it has not been addressed theoretically. One should point out that the well-known depression of critical temperature of Nb with film thickness leads to an additional suppression of the bottom layer nucleation temperature.

3.1. *Triangular wire arrays*

As an illustration Fig. 1 shows a micrograph of a superconducting triangular Nb wire network

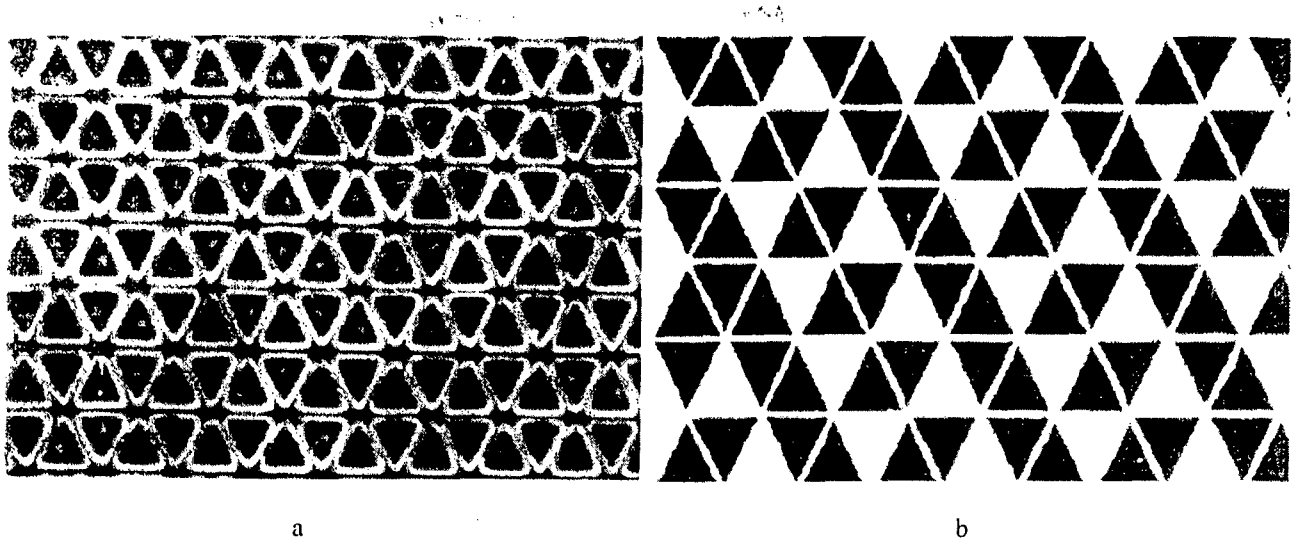

a b

Fig. 1. (a) micrograph of a triangular network of Niobium filaments after decoration by Nickel particles at frustration $f = \frac{2}{3}$. Vortex positions are visualized as clusters of Nickel particles (white spots). The long-range order in the vortex configuration is made more apparent in (b) where black triangles represent cells occupied by a vortex. The flux compression method has been used.

decorated by magnetic particles at frustration $f = \frac{2}{3}$. The sample was patterned by e-beam lithography and incomplete reactive ion etching. The width and thickness of the wire are respectively 400 and 200 nm while the residual layer in the bottom of the film is 60 nm. Separate measurements on reference samples have shown that T_C of the bottom layer is shifted down by about 0.2 K as compared to the thicker wires.

Vortex positions are visualized as clusters of Ni particles (white spots). We note that the white spots are sharp and are located near the center of the triangles. This is to be contrasted with previous experiments where the Nickel clusters were spread over the whole cells. The long-range order in the vortex configuration is made more apparent in Fig. 1(b) where black triangles represent cells occupied by one vortex. Theoretical predictions and experimental support for this stripped phase were given and discussed by Théron et al. [15] for triangular Josephson junction arrays.

3.2. Hole arrays

With increasing the width of superconducting strands the one-dimensional character of the wires is lost and a new situation occurs where vortices can exist inside the wire (except at very low frustration $f \ll 1$). Let us consider firstly a regular array of small holes at a frustration larger than unity as shown in Fig. 2. When holes are close to each other the vortex ground state is similar to that of the wire network: a commensurate lattice of vortices is observed for rational frustration [13, 14]. Fig. 2(a) shows the vortex configuration near frustration $f = 2.6$. As can be seen the holes contain either 2 or 3 vortices. There is no interstitial vortex. There is an interesting cross-over when the hole size decreases. Fig. 2(b) shows the vortex configuration for an array with the same parameters except for the smaller hole radius. Here the same frustration $f = 2.6$ leads to a quite different configuration where each hole contains 2 vortices and the extra vortices occupy intersticial positions outside the holes. The number of vortices captured in each hole is believed to be determined by the orbital quantum number of edge superconducting states. This new vortex configuration should lead to interesting dynamical properties observable in magnetization or transport measurements since intersticial vortices have a much smaller pinning force. The transition between the two states represented in Fig. 2(a) and (b) defines a first-order transition line which obviously neeeds more detailed discussion [13]. The case of low frustration ($f < 1$) is qualitatively different: in equilibrium all vortices are always trapped inside

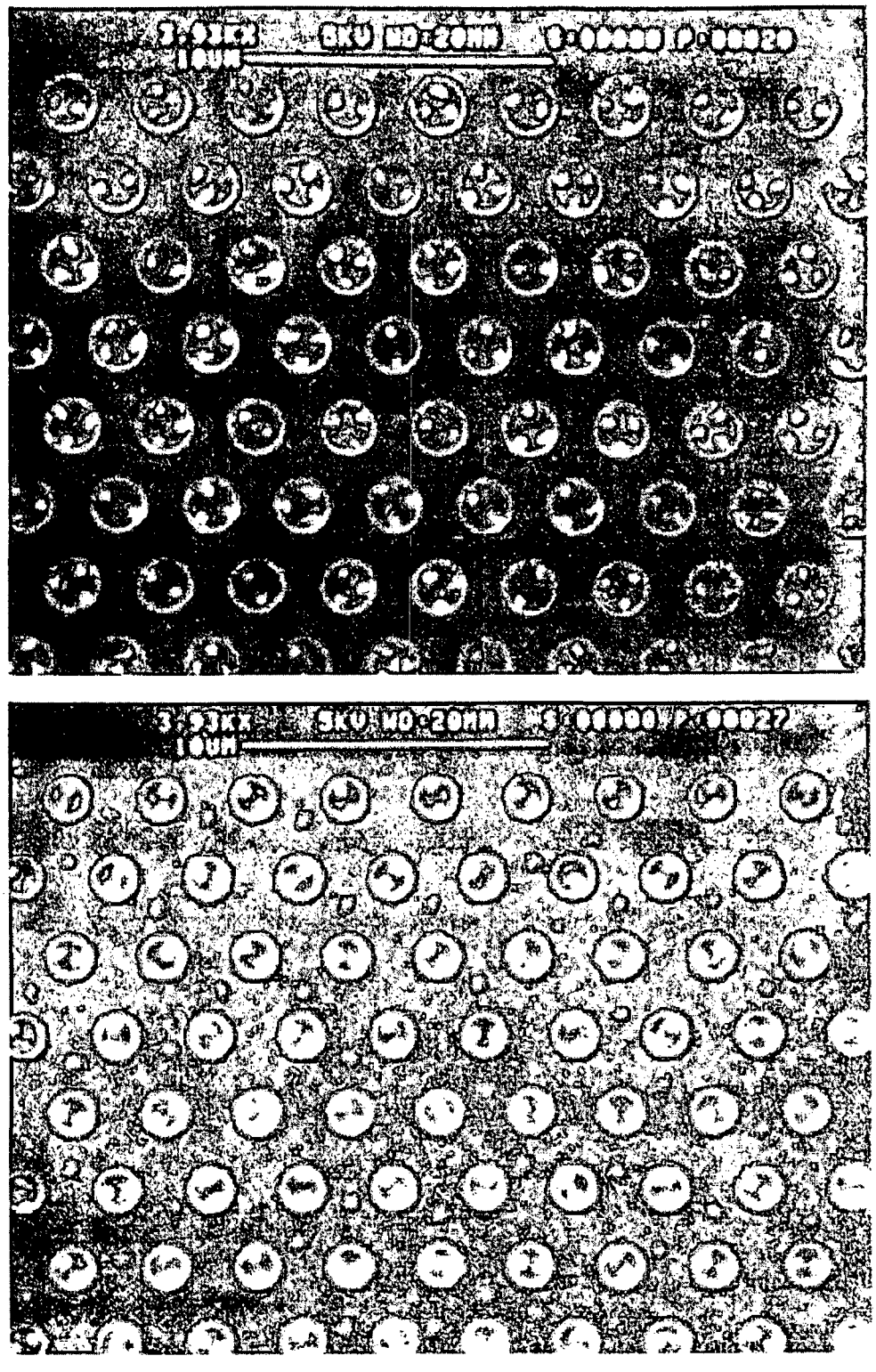

Fig. 2. Micrograph of two parts of the same sample with arrays of holes of slightly different radius: $R = 0.83$ μm (a) and $R = 0.6$ μm (b). The distance between holes in both cases is $a = 3.2$ μm. A decrease of the hole radius leads to the transition from the "collective-state" (a) where the average filling factor is equal to the frustration of the network of holes into the "single-object" state (b) when the holes are independent and capture the same number of vortices. The decoration was made after cooling at $H = 6.37$ Oe down to $T_{dec} = 4.2$ K. The vortices are visible as white spots.

holes. The decrease of the hole radius can lead only to a change in the type of the vortex (or vacancies) superlattice. For example when $\frac{3}{5} < f < \frac{2}{3}$ we have found (at the same fixed frustration) domains of a stripped face with $f = \frac{3}{5}$ in case of a large hole radius, and domains of the triangular (Abrikosov) superlattice of vacancies with $f = \frac{2}{3}$ in an arrays of small holes [14].

3.3. Other arrays

The method of flux compression has also interesting applications to other types of arrays since it allows to count number of vortices in each cell. For example we have decorated a wire array in the shape of a Sierpinski gasket at frustration $f = \frac{3}{8}$. The Sierpinsky gasket is the prototype of self-similar arrays with well-known fractal and spectral dimensions [16, 17]. It contains triangular cells of successive areas 1, 4, 16, 64 and 256. Our decoration experiment showed that the number of vortices in the corresponding stages was respectively 0, 1, 5, 22, 95, ... We have also decorated large size square and triangular SS'S Josephson junction arrays made of thick niobium islands on a thin niobium plane [18]. The decoration was successful in showing well-defined point-like vortices in the center of the cells and should bring soon precise data on very well characterized systems [15].

4. Ground state of periodic wire arrays: review of experimental results

Up to now, only three methods have been successful in imaging the ground state configurations of superconducting arrays: scanning squid [20] or Hall [19] microscopy and magnetic decoration [12]. Square Nb wire networks were studied in the three experiments. These techniques have shown similar results although each one has its own specificity.

The scanning squid microscope exhibits extremely high magnetic flux sensitivity ($10^{-5}\ \phi_0$), large scanning range (1 cm) and moderate spatial resolution (10 μm) as determined by the SQUID loop size. The corresponding field sensitivity is 210^{-6} G. The scanning Hall microscope has a lower field sensitivity (0.3 G) but higher spatial resolution (0.35 μm, scanning range a few micrometers). Both methods give access to the sign of magnetic flux: near zero external magnetic field vortex–antivortex pairs have been observed [20, 19].

The decoration method has a lower magnetic sensitivity (decoration has been successful in magnetic fields down to about one G. It has an excellent spatial resolution (better than 0.1 μm) and a large spatial range of observation since the observation is made in a standard room temperature electron microscope. Many samples can be decorated in the same run thus making the method appropriate for comparative studies of networks in the same field and temperature conditions. Magnetic particles have typical size of a few nm, the field generated by the magnetic clusters is extremely weak and was not found to produce any observable effect on the superconducting properties of the array.

All three experiments have been carried out in the freezed vortex state, i.e. well below the characteristic temperatures for vortex nucleation and motion. Hallen et al. [19] have compared the vortex pattern before and after thermal cycling near T_C. They found that thermal motion of vortices takes place between T_C and the freezing temperature which is of order of 8.7 K for their niobium networks.

Let us summarize here the main features of the vortex pattern as observed in square Nb wire networks:

(i) The vortex lattice strongly differs from the Abrikosov triangular lattice; its symetry is determined by the frustration f.
(ii) The observed configurations have the symetry $f \to 1 - f$ with respect to $f = \frac{1}{2}$.
(iii) Near a rational ($f = p/q$) the vortex lattice forms domains separated by domain walls. Domains can be very large for low rational frustrations ($f = \frac{1}{2}, \frac{2}{5}$) [12].
(iv) At low f the lattice appears very disordered. The detailed configuration changes from one observation to the other: two simultaneous decorations on identical networks or two successive scanning of the same sample separated by a thermal cycling lead to different

realizations. However the typical size and symetry of domains is the same.

(v) Near $f = \frac{1}{2}$ checkerboard domains contain vacancies and interstitial vortices: These vacancies show no long-range order.

These results are in qualitative agreement with the theoretical predictions. The configuration of vortices in superconducting arrays was first investigated by Teitel and Jayaprakash [21] and by Halsey [22]. An interesting review was given recently by Straley and Barnett [23] who made a classification of the different family of vortex states in a square Josephson array as function of frustration. A different point of view was taken by Wang et al. [24] who generalized the Abrikosov calculation of vortex lattice in type II superconductors to the wire network. This approach gave essentially the same conclusion for the low rational frustrations.

The first family is made of states $f = 1/q$ where vortices form a Bravais lattice having unit cell of size q. These lattices are deformation of the triangular Abrikosov lattice that would form in a homogeneous type II superconductor. A shear deformation is necessary to match the triangular lattice to the square network. In fact, as discussed above, the observed vortex patterns show disordered configuration presumably due to the small energy difference between different configurational states.

The second classification level is called "interpolated configurations". The patterns consist of narrow domains of Bravais lattices separated by oblique walls along the diagonal directions. In such states domains and domain walls have different vortex densities. The Halsey "staircase states" belong to this family. The observed stripped phase for $f = \frac{1}{3}$ and $\frac{2}{5}$ confirms the existence of these states. In the triangular array the stripped phase was predicted for a large range of frustration between $f = \frac{1}{3}$ and $f = 0.468$ [15]. Indeed Fig. 1 is a clear illustration of this configuration.

When approaching $f = \frac{1}{2}$, it is predicted that a checkerboard pattern with an ordered lattice of vacancies has lower energies that the Halsey states. The observed disordered arrangement of vacancies suggests that again the energy separation between different configurational states is not large enough for ordering of vacancies.

5. Conclusion

The methods of visualization have clearly made excellent progress in the last few years. The actual experimental information is still insufficient. Only few experiments have been successful in providing vortex ground state configuration and the results available so far are restricted to static properties. Many questions still remain unsolved. In the future new experiments will be needed to investigate dynamical properties. Some dynamical properties of JJ arrays under a driving current have already been investigated by Lachenmann et al. [25]. The low-temperature scanning electron microscope method uses local perturbation of the Josephson current to probe the voltage induced by vortex motion. Although the typical time scale of vortex dynamics is certainly extremely high some dynamical regime should be attainable by the present scanning or holography methods [26].

Acknowledgements

We are very grateful to M. Ferlet for help in the decoration experiments. We thank P. Martinoli for useful discussions. This work was supported by the CEE "SUPNET" contract ERBCGRCT920068.

References

[1] H.F. Hess, R.B. Robinson, R.C. Dynes, J.M. Valles Jr. and J.V. Waszczak, Phys. Rev. Lett. 62 (1989) 214.
[2] I. Maggio-Aprile, Ch. Renner, A. Erb, E. Walker and O. Fisher, Phys. Rev. Lett. 75 (1995) 2754.
[3] H. Trauble and U. Essmann, J. Sci. Instr. 43 (1966) 344.
[4] P.L. Gammel, D.J. Bishop, G.J. Dolan, J.R. Kwo, C.A. Murray, L.F. Schneemeyer and J. Waszczak, Phys. Rev. Lett. 59 (1987) 2593.
[5] D.J. Bishop, P.L. Gammel, D.A. Huse and C.A. Muray, Science 255 (1992) 165.
[6] Zhen Yao, Seokwon, Yoon, Hongjie Dai, Shoushan Fan and Charles M. Lieber, Nature 371 (1994) 777.
[7] C. Tsuei, J.R. Kirtley, C.C. Chi, L.S. Yu-Jahnes, A. Gupta, T. Shaw, J.Z. Sun and M.B. Ketchen, Phys. Rev. Lett. 73 (1994) 593.

[8] A. Moser, H.J. Hug, I. Parashikov, B. Stiefel, O. Fritz, H. Thomas, A. Baratoff, H.J. Guntherodt and P. Chaudhari, Phys. Rev. Lett. 74 (1995) 1847.
[9] K. Haralda, T. Matsuda, H. Kasai, J.E. Bonewitch, T. Yoshida, U. Kawabe and A. Tonomura, Phys. Rev. Lett. 71 (1993) 3371.
[10] C.J. Lobb, Physica B 152 (1988) 1.
[11] C.J. Lobb, D.W. Abraham and M. Tinkham, Phys. Rev. B27 (1983) 150.
[12] K. Runge and B. Pannetier, J. Phys. I 3 Colloque Rammal (1993) 389; Europhys. Lett. 24 (1993) 389.
[13] A. Bezryadin and B. Pannetier, J. Low Temp. Phys. 102 (1996) 73. A. Bezryadin, Y. Ovchinikov and B. Pannetier, Phys. Rev. B, to appear.
[14] A. Bezryadin, A. Buzdin and B. Pannetier, Proceedings of "Macroscopic Quantum Phenomena and Coherence in Superconducting Networks", ed. C. Giovanella (World Publ. Co., New York, 1995).
[15] R. Théron, S.E. Korshunov, J.B. Simon, C.H. Lehmann and P. Martinoli, Phys. Rev. Lett. 72 (1994) 562.
[16] R. Rammal and G. Toulouse, Phys. Rev. Lett. 49 (1982) 1194.
[17] R. Meyer, J.L. Gavilano, B. Jeanneret, R. Theron, Ch. Leemann, H. Beck and P. Martinoli, Phys. Rev. Lett. 67 (1991) 3022.
[18] A. Eichenberger, A. Bezryadin, P. Martinoli and B. Pannetier, to be published.
[19] H.D. Hallen, R. Seshadri, A.M. Chang, R.E. Miller, L.N. Pfeiffer, K.W. West, C.A. Murray and H.F. Hess, Phys. Rev. Lett. 71 (1993) 3007; A.M. Chang, H.D. Hallen, L. Harriott, H.F. Hess, H.L. Kao, J. Kwo, R.E. Miller, R. Wolfe, J. Van der Ziel and T.Y. Chang, Appl. Phys. Lett. 61 (1992) 1974.
[20] L.N. Vu, M.S. Wistrom and D.J. Van Harlingen, Appl. Phys. Lett. 63 (1993) 1693.
[21] S. Teitel and C. Jayaprakash, Phys. Rev. Lett. 51 (1983) 1999.
[22] T. Halsey, Phys. Rev. B 31 (1985) 5728.
[23] J.P. Straley and G.M. Barnett, Phys. Rev. B 48 (1993) 389.
[24] Y.Y. Wang, R. Rammal and B. Pannetier, J. Low Temp. Phys. 68 (1987) 301.
[25] S. Lachenmann, T. Doderer, D. Hoffmann, R.P. Huebener, P.A.A. Booi and S.P. Benz, Phys. Rev. B 50 (1994) 3158.
[26] Y. Otani, K. Runge, T. Matsuda and A. Tonomura, unpublished.

Vortex dans un réseau supraconducteur sous champ magnétique

B. Pannetier [1] ***and A. Eichenberger*** [2]
[1] *CNRS-CRTBT, BP 166, 38042 Grenoble Cedex 9 France*
Laboratoire associé à l'Université J. Fourier
[2] *Institut de Physique, Neuchâtel, CH-2000 Suisse*

Abstract: *Here we present the results of a direct observation by Bitter decoration of vortices in an artificial superconducting network. As expected, the observed vortex configuration in a periodic network is highly sensitive to the magnetic frustration. Large domains of vortex commensurate states are detected in the neighbourhood of frustrations 1/2, 1/3 and 2/5. These results are analysed in relation to the ground state models.*

Résumé: *Nous présentons les résultats d'une expérience d'observation directe par décoration de Bitter des vortex dans un réseau supraconducteur artificiel. Comme attendu, la configuration observée dans un réseau périodique est sensible à la frustration magnétique. De grands domaines commensurables sont mis en évidence au voisinage des frustrations 1/2, 1/3 et 2/5. Ces résultats sont analysés en fonction des modèles de l'état fondamental.*

Introduction

Le réseau supraconducteur constitue un système modèle d'excellence pour l'étude de l'organisation complexe de la fonction d'onde dans un système frustré puisque la frustration peut être ajustée d'une façon précise et continue à l'aide d'un faible champ magnétique. La frustration est définie comme le flux magnétique réduit $f=\phi/\phi_0$, où ϕ est le flux magnétique traversant la plaquette élémentaire du réseau et $\phi_0 = h/2e$ est le quantum de flux supraconducteur. Le réseau supraconducteur en tant que système modèle a été introduit à l'origine comme une modélisation de matériaux supraconducteurs très désordonnés [1, 2, 3] , le désordre donnant lieu à une structure percolative essentiellement hétérogène. Une réalisation pratique simple de ces systèmes est le réseau périodique de filaments supraonducteurs. Les propriétés supraconductrices reflètent fidèlement la topologie du réseau et apportent des informations originales et uniques sur les niveaux de Landau dans un système périodique [2]: Par exemple la ligne de transition de phase Tc(H) [4] est une ligne fractale qui coincide avec le bord du spectre de Hofstadter [5] et la courbe d'aimantation est une suite de sauts d'aimantation aux valeurs rationelles de la frustration[6]. Ces sauts s'interprètent comme une manifestation de la phase de Berry [7]. La compréhension théorique de ces propriétés, bien confirmées par l'expérience, repose sur la description de la configuration de la fonction d'onde supraconductrice en super réseau pour les "frustrations rationelles" f=p/q ou p et q sont des nombres entiers. Bien que cette description soit bien admise à l'heure actuelle, on en a encore aucune confirmation directe, on a

également très peu d'information sur l'influence des dégénérescences, défauts et parois de domaines qui jouent un grand rôle dans les propriétés dynamiques du réseau.

Nous avons développé une technique d'observation directe de la répartition spatiale du réseau de vortex[8]. Celle-ci permet une représentation fidèle de la configuration de la fonction d'onde. Nos premiers résultats confirment l'existence d'un ordre très sensible à la frustration dans le réseau de vortex. Une alternative au réseau de fils est le réseau de jonctions Josephson qui constitue une autre limite (limite de couplage faible) de système supraconducteur hétérogène: la physique est similaire et peut être décrite à l'aide du modèle X-Y frustré.

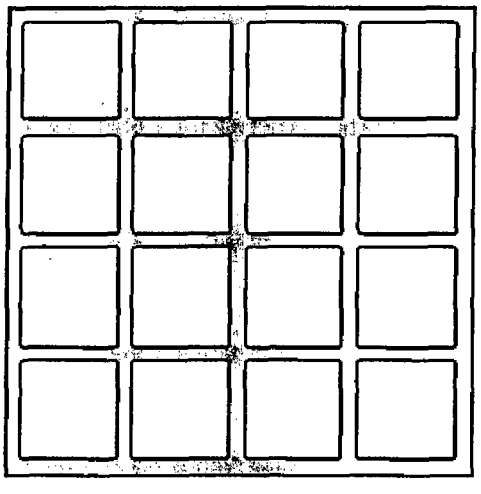

Figure1- Représentation schématique d'un réseau de filaments supraconducteurs. En pratique le réseau est réalisé par gravure ionique réactive d'une couche épitaxiée de niobium d'épaisseur 200nm. La largeur typique des filaments est w=400nm et le pas du réseau a=3 μm.

La configuration de l'état de vortex d'un supraconducteur homogène de type II, a été déterminée par Abrikosov [9] en 1957. La méthode, qui consiste à minimiser l'énergie libre de Ginzburg-Landau a été généralisée au réseau supraconducteur par Wang et al. [10] en 1987. Le réseau Josephson a été étudié par différents auteurs [11-13] par des méthodes de Monte Carlo. Les points communs à ces différentes études sont analysés dans l'article de Straley et Barnett [13] où sont classifiés les différentes familles d'états commensurables dans un réseau carré infini: Les symétries permettent de réduire la zône d'étude à l'intervalle f={0,1/2} entre l'état uniforme à f=0 et l'état en échiquier à f=1/2. Pour f petit le réseau de vortex, peu dense, est une déformation du réseau triangulaire d'Abrikosov. Aux valeurs intermédiaires les différents modèles prédisent une structure en escalier formée d'une succession de domaines obliques. Près de f=1/2 l'état de plus basse énergie est un échiquier contenant un super réseau ordonné de lacunes. L'analyse du réseau triangulaire de jonctions Josephson a été faite récemment par R. Théron et al. [14]. Dans ce travail les mesures de réponse superfluide ont permis de mettre en évidence une suite d'états

commensurables formés de domaines linéaires de même nature que les phases en escalier présentées ci-dessus.

Expériences et discussion

L'imagerie des vortex dans les supraconducteurs a bénéficié du développement de nombreuses techniques à très haute résolution spatiale et magnétique. Très peu d'entre elles [8,15] ont pu être appliquées aux réseaux supraconducteurs du fait des contraintes spécifiques liées à la nature des vortex dans ces systèmes. En effet le vortex n'a pas de coeur et son extension spatiale est définie par la taille d'une cellule du réseau et non par les longueurs charactéristiques microscopiques (longueur de pénétration magnétique et longueur de cohérence supraconductrice); de plus la faiblesse du couplage supraconducteur entre les noeuds du réseau réduit considérablement l'écrantage et le contraste magnétique. Une particularité supplémentaire est le très fort piégeage par les fils du réseau. La méthode de Bitter classique est simple [8], possède à la fois une très haute résolution spatiale et un grand champ d'observation. En revanche elle a en général une relativement faible sensibilité vis-à-vis du champ magnétique et demande une adaptation.

Notre optimisation repose sur les points suivants:

- Puisque le système est extrêmement sensible au flux magnétique et que le caractère rationnel de la frustration est critique, le choix de f nécessite une bonne compensation du champ magnétique résiduel et une bonne calibration du champ. En général une mesure *in situ* de la magnétorésistance permet de repérer les pics de commensurabilité et de fixer très précisément le champ magnétique à la valeur choisie. Le réseau est ensuite refroidi très lentement au-dessous de la transition. A température suffisament basse (quelques dizaines de millikelvin au dessous de la température de transition), les vortex perdent leur mobilité et restent piégés par la structure du réseau. La décoration proprement dite est effectuée à basse température lorsque la configuration est gelée.
- La variation du champ magnétique au voisinage d'un réseau de fils s'exprime à l'aide d'un facteur de contraste défini comme la différence de champ entre cellules avec vortex et cellules sans vortex. Dans le cas idéal où la largeur des fils est supérieure à la longueur de pénétration magnétique, la quantification du flux est satisfaite, ce facteur de contraste vaut alors ϕ_0/a^2 où a est le pas du réseau. En pratique ce facteur est réduit en proportion du rapport s/λ^2 (s section du fil). Compte-tenu de la taille des cellules a Å 1.m, le contraste de champ est, dans tous les cas, de plusieurs ordres de grandeur inférieure au contraste de champ ϕ_0/λ^2 près d'un vortex dans un supraconducteur homogène. Le choix de filaments de Niobium épitaxié sous

ultravide et "découpé" par gravure ionique réactive nous a permis d'atteindre un contraste magnétique de l'ordre du mT. Les premières observations de vortex dans un réseau carré ont été réalisées de cette manière [8] mais sont en pratique très délicates à mettre en oeuvre de façon reproductible.

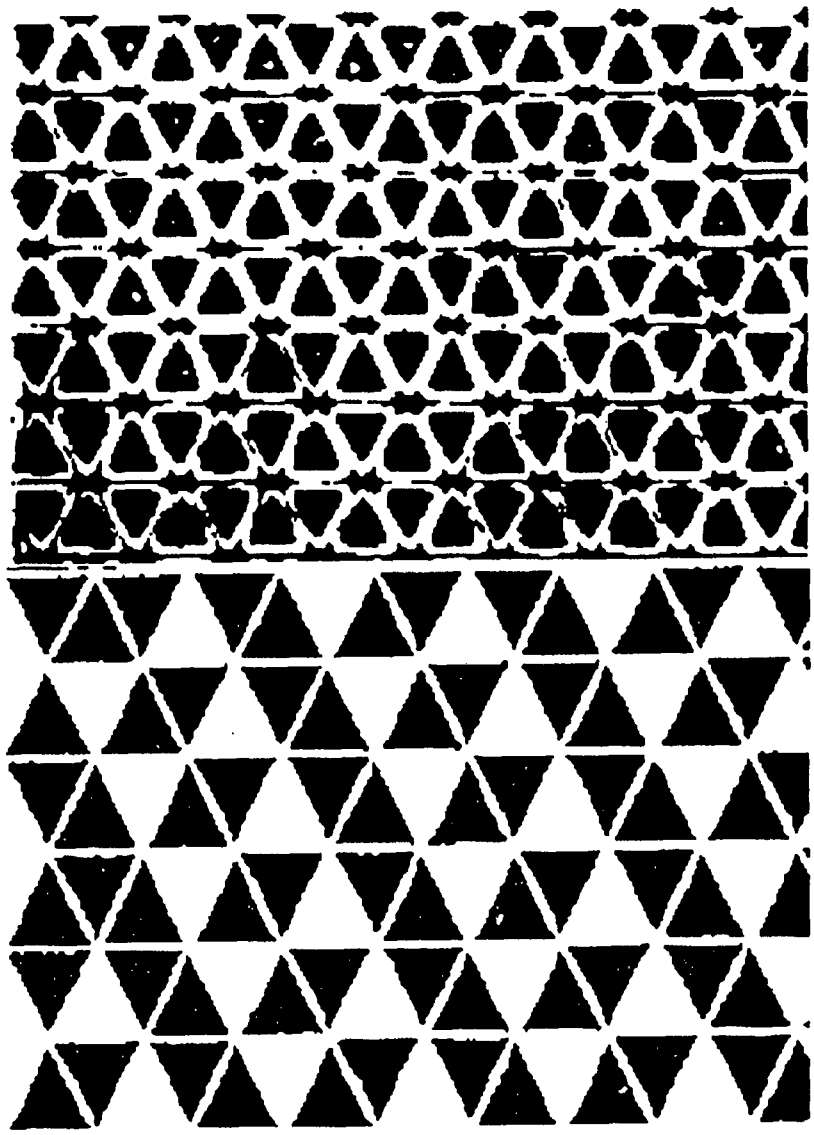

Figure 2: En haut: Micrographie d'un réseau triangulaire de filaments de niobium après décoration par des particules de Nickel à frustration f=2/3. La position des vortex est marquée par les amas (points blanc) de particules de nickel situés au milieu des cellules du réseau. La méthode de compression de flux[17] a été utilisée dans cette décoration. En bas: L'ordre à longue distance est rendu apparant dans une représentation où les triangles noirs marquent les cellules occupées par un vortex. Il s'agit ici de la phase en escalier attendue pour l'état 2/3.

- une nouvelle méthode d'amélioration du contraste a permis récemment d'atteindre une excellente reproductibilité. Le principe repose sur une

méthode de compression de flux magnétique [17] dans laquelle une couche mince supraconductrice additionnelle placée sous le réseau permet le "marquage" des vortex. On retrouve alors le contraste magnétique optimum ϕ_0/λ^2 . En pratique la méthode de préparation consiste à interrompre la gravure ionique de façon à laisser une couche résiduelle de niobium d'épaisseur non nulle (60 nm) au fond des cellules.

Comme illustration, la Figure 2 montre un réseau triangulaire de Niobium après décoration à frustration f=2/3. Les vortex apparaissent comme des points clairs situés au milieu de certains triangles. La décoration a été faite par la méthode de compression de flux. On observe clairement la phase ordonnée de type escalier attendue pour l'état 2/3. Des expériences similaires ont été réalisées en fonction de la frustration dans des géométries de réseaux très variées: réseaux carrés, réseaux triangulaires, réseaux fractals (tamis deSierpinski), réseaux de jonctions Josephson [18], réseaux de trous [17].

Nous résumons ici les principales observations dans le cas d'un réseau carré périodique:

- Le réseau de vortex n'est pas triangulaire: il est déterminé par la frustration **f**.
- les configurations observées sont symétriques vis-à-vis de f=1/2.
- pour **f** voisin d'un rationnel, les vortex forment des domaines séparés par des parois de domaines. Les domaines sont très grands (plusieurs dizaines de cellules) pour f=1/2 ou 2/5.
- Pour **f** petit le réseau apparaît très désordonné quelle que soit la méthode d'observation (décoration magnétique [8] ou microscopie magnétique à balayage [15]).
- Près de f=1/2, les domaines en échiquier contiennent des lacunes qui ne présentent pas d'ordre à longue distance.
- La configuration précise change d'une observation à l'autre: deux observations simultanées sur deux échantillons identiques, ou deux observations d'un même échantillon séparées par un recyclage thermique, donnent des réalisations statistiques différentes. Cependant la taille et la symétrie des domaines restent identiques. Les expériences réalisées par microscopie magnétique à balayage [15] montrent que le réseau de vortex reste immobile tant que la température est inférieure 8.7K (Tc=8.8K) pour un réseau de filaments de niobium.

Conclusion

Nous avons montré qu'il est possible de mettre en évidence de façon directe la configuration des vortex dans un réseau supraconducteur. Les premiers résultats montrent l'existence de domaines de grande taille confirmant la

structure de l'état fondamental pour les rationnels simples. Ces domaines constituent une manifestation directe de l'ordre spatiale de la fonction d'onde qui avait été proposée dans les tout premiers travaux théoriques [2] sur ces systèmes. Le champ d'étude des réseaux supraconducteurs s'est enrichi récemment d'effets physiques nouveaux liés à la nature quantique des vortex dans les systèmes de très petite taille [19]. Il est clair que les méthodes d'observation spatiales apporteront beaucoup dans les années qui viennent à la compréhension physique de ces systèmes modèles.

Remerciements

Ce travail a bénéficié du soutien de la Communauté Européenne sous le contrat n° CHRX-CT92-0068. Il a été mené dans le cadre du programme "réseaux supraconducteurs" initié au Centre de Recherches sur les Très Basses Températures du CNRS Grenoble sous l'impulsion de R. Rammal. Les auteurs tiennent à rendre un hommage appuyé au rôle précurseur joué par R.Rammal dans la compréhension théorique de ces systèmes modèles et à souligner le bénéfice immense qu'il a apporté à la communauté scientifique grâce notamment à sa relation exemplaire avec la physique expérimentale.

Références

1. De Gennes P.G.,1981. C.R. Ac. Sci. B292, 9 et 279.
2. Rammal R., Lubensky T.C., and Toulouse G.,1983. *Phys. Rev.* B27, 2820.
3. Alexander S.,1983. *Phys. Rev.* B27, 1547.
4. Pannetier B., Chaussy J., and Rammal R.,1984. *J. Phys. Lett.* 44 L853 (1983); *Phys. Rev. Letters*, 53,01845.
5. Hofstadter D.R.,1976. *Phys. Rev.* B14, 2239.
6. Gandit P., Chaussy J., Pannetier B., Vareille A., and Tissier A.,1987. *EuroPhys Lett.* 623.
7. Rammal R., 1988. *Physica* B152, 37.
8. Runge K. et Pannetier B.,1993. J. Phys. 13 , Colloque Rammal, p. 389;1993. *Europhys. Letters* 24, p. 389.
9. Abrikosov A.,1957. Sov. Phys. JETP5, p1174
10. Wang Y.Y., Rammal R., and Pannetier B.,1987. *J. Low Temp.* Phys. 68, 301.
11. Teitel S. and Jayaprakash C.,1983. *Phys. Rev. Lett.* 51, 1999.
12. Halsey T.C., 1985. *Phys. Rev.* b31, 5728
13. Straley J.P. and Barnett G.M., 1993. *Phys. Rev* B48, 389
14. Théron R., Korshunov S.E., Simon J.B., Lehmann CH., and Martinoli P.,1994. *Phys. Rev. Letters* 72, 562
15. Hallen H.D. et al.,1993. Phys. Rev. Letters 71, 3007; Vu L.N. et al. 1993. *App. Phys. Letters*, 1693.
16. Traüble H. and Essmann U.,1996 J. Sci. Instr. 43, 344.
17. Bezryadin A. and Pannetier B.,1995. *J. Low Temp. Phys.* à paraitre.
18. Eichenberger A. et al , non publié.
19. Voir par exemple H.J. Mooij and G.Schön, 1992. dans "*Single Charge Tunneling,*" NATO ASI series, Plenum Volume 294, Ed. H. Grabert and M. Dévoret.